Tungsten transport in tokamaks: towards real-time kinetic-theory-based plasma performance optimisation

P. Manas, C. Angioni, E. Fable, C. Stephens, J.-F. Artaud, C. Bourdelle, P. Maget, J. Citrin, K. van de Plassche, F. Felici, et al.

TUNGSTEN TRANSPORT IN TOKAMAKS: TOWARDS REAL-TIME KINETIC-THEORY-BASED PLASMA PERFORMANCE OPTIMISATION

P. MANAS
CEA, IRFM, F-13108
Saint Paul-lez Durance, France
Email: pierre.manas@cea.fr

C. ANGIONI, E. FABLE, C. STEPHENS
Max-Planck-Institut für Plasmaphysik, D-85748
Garching, Germany

J.F. ARTAUD, C. BOURDELLE, P. MAGET
CEA, IRFM, F-13108
Saint Paul-lez Durance, France

J. CITRIN, K. VAN DE PLASSCHE
DIFFER-Dutch Institute for Fundamental Energy Research
Eindhoven, the Netherlands

F. FELICI
Ecole Polytechnique Federale de Lausanne (EPFL), Swiss Plasma Center (SPC), CH-1015
Lausanne, Switzerland

X. YANG
Institute of Plasma Physics, Chinese Academy of Science
Hefei, China

the ASDEX Upgrade Team
H. Meyer et al, Nuclear Fusion 59 (2019) 112014

and the WEST Team
http://west.cea.fr/WESTteam

Abstract

Mechanisms by which tungsten dynamically accumulates in the core of tokamaks are identified in integrated modelling of an ASDEX-Upgrade discharge. Then the same modelling tools are applied to a WEST long pulse L-mode plasma. This modelling work on two disctinct tokamaks also stresses the validaty domain of reduced transport models, in this case QuaLiKiz. At AUG, a ramp-down of the Electron Cyclotron Resonance heating is analysed with a constant background Neutral Beam Injection heating until W accumulation is observed. It is found that the central ratio of the electron to the ion temperature, together with the central source of particles deposited by the beams play a key role. Indeed, while the central particle source yields more centrally peaked density profiles, leading to inward neoclassical convection of tungsten, large Te/Ti can compensate this unfavorable scenario by increasing turbulent particle diffusion. Such competition between Te/Ti and the central particle source is also investigated with fast transport models, in particular within the integrated modelling framework RAPTOR where the turbulent transport is computed from QuaLiKiz 10D neural network. This paves the way towards real-time-kinetic-theory-based plasma performance optimisation. Finally, modelled WEST plasmas with dominant electron heating showed the limits of the implemented collision operator in QuaLiKiz yielding an overstabilisation of Trapped Electron Mode, resulting in mispredictions of the kinetic profiles (electron density and temperature).

INTRODUCTION

Tungsten is foreseen as plasma facing material in next generation tokamaks (ITER/DEMO) due to better properties: high melting point, capable of sustaining high heat and particle fluxes from the core, low erosion rates and limits the fuel retention which is, in particular, relevant to prevent radioactive tritium accumulation in the wall components. In view of these overall good qualities and the need to gather experience on tokamak operation with W plasma facing components, in Europe AUG and JET have been already operated for several campaigns with a full W wall and a W divertor respectively, and WEST is recently operating with a W wall as well. Experiments in AUG and JET have shown that the presence of W significantly affects plasma operation,

limits the routinely achievable parameter domain of the device and requires actions to avoid central accumulation, which leads to high levels of core radiation due to the high charge number and partial ionisation. Uncontrolled central W accumulation produces large radiation losses and can trigger the loss of the high confinement regime (H-mode) or even disruptions, which are both detrimental for ITER (marginal input power with respect to the L-H transition power threshold and severe damages caused by disruptions).

For these reasons it is necessary to predict such detrimental scenarios regarding W accumulation in the plasma core. For such predictions, integrated modelling frameworks are required, not only to predict W transport but also the evolution of the electron density and ion/electron temperature profiles to resolve the nonlinear interactions among all transport channels. These frameworks necessitate accurate models for turbulent and neoclassical transport, but also suficiently fast models to prepare plasma scenarios prior to operation or even control the W accumulation in real time. In this work, we analyse W accumulation in an ASDEX Upgrade discharge within the integrated modelling framework ASTRA to underline the dominant ingredients in developing such accumulations. Then faster transport models are benchmarked on such cases, in particular the turbulent transport from QuaLiKiz-10D neural network within the integrated modelling platform RAPTOR.

Then the same tools are used to model tungsten transport in a WEST long pulse L-mode. The absence of toroidal rotation sources, the large aspect ratio and dominant electron heating allows us to stress the predictive capabilities of the transport models used in view of extrapolation to future reactors, in particular the first pre-fusion power phase of ITER. In this case, mispredictions are found due to overstabilisation of Trapped Electron Mode by collisions. To characterise this behaviour, the flux driven simulations performed so far are also complemented with gradient driven simulations.

First in section 1.1, the experimental setup for the ASDEX Upgrade H-mode featuring a tungsten accumulation is described. In particular, the discharge analysed features a ramp-down of the ECRH power. In section 1.2 the assumptions used in the integrated modelling framework ASTRA are described. Then dominant ingredients found responsible for W accumulation are underlined, namely the central particle source from the neutral beams and the central ratio Te/Ti. Faster transport models are also qualitatively validated with respect to mechanisms described above. Finally in section 2, a WEST long pulse L-mode plasma is described where tungsten does not accumulate throughout the 33 seconds of the discharge. Flux driven and gradient driven simulations are performed to characterise the mispredictions obtained in the regime of dominant electron heating.

1. TUNGSTEN ACCUMULATION IN ASDEX UPGRADE NBI HEATED H-MODE PLASMA

1.1. Experimental setup

A particular ASDEX-Upgrade discharge featuring a ramp-down of the ECRH power is studied in the following, where previous analyses of tungsten accumulation were performed for steady phases [1, 2]. It consists of an H-mode plasma with Ip = 1 MA, BT = 2.5 T, ne =9 x 10^{19} m-3, 7.5 MW of injected NBI power. Here we focus on two time windows where PECRH = 200 kW and PECRH = 1.9 MW. The time traces of the NBI, radiated and ECRH power together with the central and mid-radius tungsten densities inferred from UV grazing incidence spectroscopy are shown in Fig. 1. It is observed that while the ECRH injected power is decreased, the central tungsten density (r/a = 0.2) is steadily increasing. On the other hand the mid-radius tungsten density is decreasing. When the ECRH power is completely switched off, a strong accumulation is observed first in the central region and then at mid-radius which causes a collapse of the electron temperature. Prior to this accumulation phase, it is also observed that the central tungsten density is increasing in between sawtooth crashes. Ion and electron temperature profiles for the two extreme phases of interest, i.e. for PECRH = 200 kW and PECRH = 1.9 MW are also gathered in Fig. 1. The electron density profiles are provided by the integrated data analysis IDA (interferometry+Thomson scattering). The toroidal Mach number and the ion temperature profiles are computed from Charge eXchange Recombination spectroscopy. The electron temperature are given by the Electron Cyclotron Emission measurements. It is shown that the the electron temperature is similar/lower than the ion temperature profile at low ECRH power. On the other hand, for the PECRH = 1.9 MW case, the ratio Te/Ti remains above unity in the radial domain r/a < 0.4. The role of the central electron to ion temperature ratio and the central particle peaking will be further discussed.

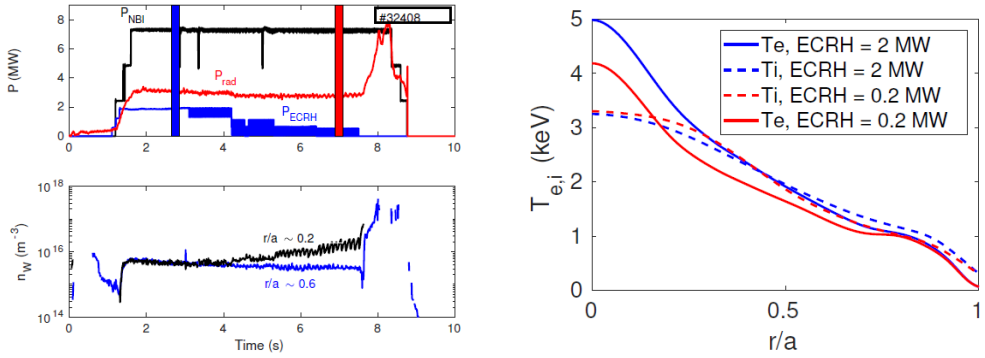

Figure 1: (left top panel) Time traces of the NBI, radiated and ECRH power for #32408. The two time windows scrutinized in the modelling section are highlighted. (left bottom panel) Time traces of the two radial locations of the W density reconstructed from the UV grazing incidence spectroscopy. (right) Ion and electron temperatures for the two time windows, at high and low ECRH injected power.

1.2. Integrated modelling

1.2.1. Central particle source and neoclassical convection

To investigate the impact of different mechanisms on the tungsten transport within this discharge, the integrated modelling framework ASTRA [3] has been used. The turbulent transport is modelled with the linear gyrokinetic code QuaLiKiz [4] and the neoclassical transport with the code NEO [5], both including the impact of toroidal rotation on the fluxes. Regarding the heat and particle sources, the TORBEAM code is used outside the integrated modelling framework to compute the deposited power on the electons for each steady state phases.

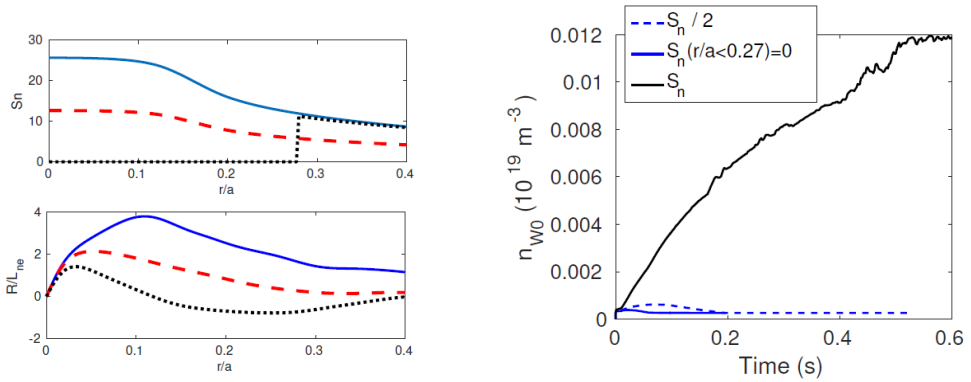

Figure 2: (left top panel) Assumptions used for the central particle source in the integrated modelling of the W accumulation phase. (left bottom panel) Resulting electron density profiles. (right) Simulated central tungsten density, using the different assumptions for the particle source.

The NBI deposited power is computed self consistently with the evolved plasma state inside the ASTRA framework, together with the particle source. The latter also includes the Ware pinch computed from NEO. The following channels are then evolved in time in the simulation: the electron temperature and density, the tungsten density, the ion temperature and the current. The toroidal rotation, though included in the simulation as measured by CXRS, is not evolving and is fixed for each steady state phases studied. The goal is to model the central accumulation or non accumulation of tungsten for a given injected ECRH power, and in particular for the two extreme phases of Fig 1. As the neoclassical convection of W is unfavourable with respect to the electron density peaking, in contrast to temperature peaking which results in the so-called thermal screening, the evolution of the electron density in the simulation is tested for different particle sources. The first assumption follows the computation from the NBI module in ASTRA, giving a centrally peaked particle source. Then a reduction of a factor 2 of this particle source has been used and finally the central part r/a < 0.27 has been switched off. The profiles of these sources are shown in Fig. 2. The resulting predicted density profiles, at

equilibrium between transport and sources, yield the central density peaking also shown in Fig. 2. It is found that the NBI central particle source is the main ingredient in setting the peaked density profiles and not the transport alone. Finally, inside r/a = 0.1, the Ware pinch is also an important ingredient as shown in the case where there is no turbulent transport nor particle sources (switched off). For the three particle source shapes described previously, the resulting central tungsten density is also predicted and shown in Fig. 2. It is found that tungsten accumulates in the simulation (up to a concentration of 10^{-3}) only when the nominal particle source is used. For the two other cases, the electron density peaking is not driving sufficiently inward neoclassical tungsten convection to trigger an accumulation. This clearly shows that the central electron density peaking and thus the particle source from the beam is the main ingredient in triggering central tungsten accumulation in this case. The role of the ECRH power regarding the onset of large electron density peaking is investigated in the following.

1.2.2. Core Te/Ti and density pump-out

The role of turbulence in developping peaked density profiles has been shown to be the main ingredient in front of the particle source. However the central accumulation problem is set up in a radial domain where turbulence is not the dominant transport process (central region inside r/a = 0.2) and where the source also becomes important. It is thus important to assess the role of turbulence at different central Te/Ti, i.e. at different injected central electron power. Integrated simulations with ASTRA and QuaLiKiz for the turbulent transport have shown that for the high ECRH power case, Electron Temperature Gradient driven instabilities were destabilised in the core. This results in large electron heat transport and thus central Te/Ti close to 1. This is in contrast to what is observed experimentally, where in the high ECRH case Te/Ti is larger than 1. Such discrepancies with experimental measurements of the ion and electron temperature profiles are shown in Fig. 3. When relaxing the quasilinear weight of ETGs in the turbulent transport, higher Te/Ti are recovered in the simulations, though the values are higher than in the experiment. This shows that a proper evaluation of the electron heat transport through the ETG instabilities have to be assessed which is a complex problem for

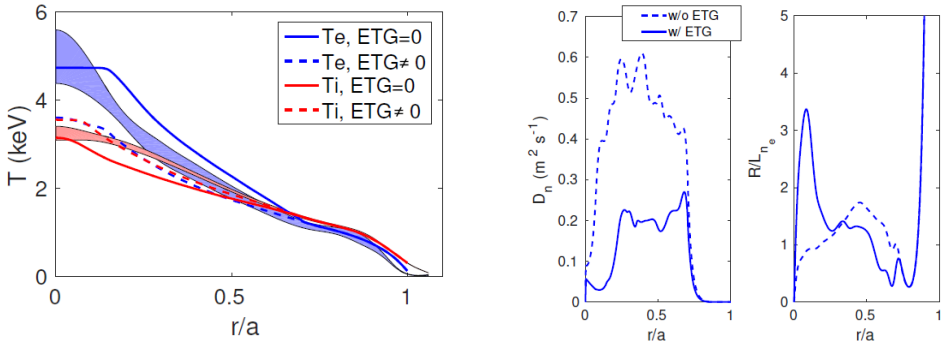

Figure 3: (left) Modelled and experimental ion and electron temperature profiles, with and without ETG contributions in the computed electron heat flux. (right) Turbulent particle diffusion and resulting central density peaking.

quasilinear codes. For a proper treatment, nonlinear multiscale gyrokinetic simulations are required which cannot be used in an integrated modelling framework. Nevertheless the impact of Te/Ti and thus of the centrally deposited ECRH power can be underlined in the simulations. Indeed, the turbulent particle diffusion together with the predicted density peaking are shown in Fig. 3 with an without ETGs electron heat transport or in other word for large/low central Te/Ti. It is found that when the central Te/Ti is large, above 1, turbulent diffusion can compensate the central particle source which results in modest central density peaking. This low density peaking is favourable with respect to central neoclassical tungsten accumulation. On the other hand, when Te/Ti is close to 1 or below, the central turbulent diffusion is reduced yielding large centrally located density peaking which in turn results in large inward tungsten neoclassical convection.

1.2.3. Fast turbulent transport model: QuaLiKiz-10D neural network

To go towards real time control of tungsten transport in tokamaks, faster models for turbulent and neoclassical transport are required while retaining as much physics as possible, e.g. toroidal rotation. In this section, a neural network of QuaLiKiz [6] is used within the integrated framework RAPTOR [7]. In this framework, the transport equations for impurity densities are not solved but the interplay between density pump-out and central particle source observed in the previous sections and responsible for tungsten accumulation is investigated. To do so, transport equations for the electron density and temperature, the main ion temperature and the current diffusion are evolved in time. The sources are taken identical to the ASTRA simulations.

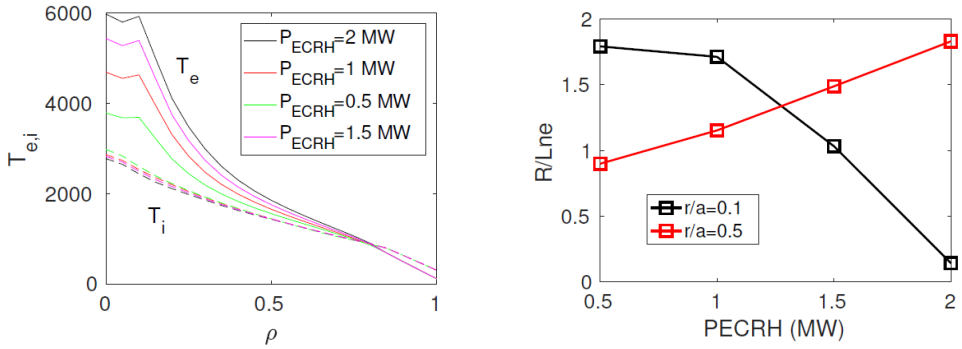

Figure 4: (left) Electron temperature profiles predicted with RAPTOR and QuaLiKiz 10D neural network. (right) Predicted electron density peakings at two radial position for various levels of ECRH power.

A scan in the injected ECRH power is then performed and the resulting temperature profiles are shown in Fig. 4. As expected, Te/Ti increases while increasing the ECRH power. The central density peaking at r/a=0.1 (also shown in Fig.4) decreases which qualitatively reproduces the density pump-out with Te/Ti observed in ASTRA. At mid-radius, on the other hand, the density peaking increases which is consistent with changes in collisionality from increasing Te [8]. Again it is to be emphasized that the coupling of the central tungsten content (accumulation) and Te through radiation is currently missing in such simulations. Nevertheless, this qualitative agreement between ASTRA/QuaLiKiz and RAPTOR/QLKZ-10DNN is promising for fast tungsten accumulation predictions.

2. WEST LONG PULSE L-MODE WITH DOMINANT ELECTRON HEATING

To stress the validity of the transport models used to predict tungsten accumulation in AUG, the same tools are used for a WEST long pulse L-mode discharge where no accumulation is observed. This also allows us to cover a wider operational domain, that is considering larger aspect ratio, absence of injected torque and central particle sources from NBI, dominant electron heating from LHCD and ICRH heating systems. These plasmas are particularly relevant considering scenarios of the Pre-Fusion Power Operation phase 1 of ITER where cyclotron resonance heating will be used (20 to 30 MW of ECRH), without neutral beams.

2.1. Experimental setup

In this WEST plasma lasting over 30 seconds, the tungsten content is monitored through UV spectroscopy, SXR, bolometry and visible spectroscopy. The magnetic field was at its nominal value of 3.7 T, in upper single null configuration, the plasma current plateau at 400 kA and up to 2.8 MW of LHCD is delivered. It is observed (time traces in Fig. 5) that tungsten does not accumulate throughout this long pulse. More details on the tungsten transport modelling for this plasma can be found in [9]. An increased in the total radiated power is observed during the ICRH heated phase but is not considered in the following analysis. Electron temperature profiles (to be compared to the modelling in the next section) are extracted from Electron Cyclotron Emission (ECE) which makes the measurements reliable only in the region r/a<0.6 due to polluted signal from LHCD non-thermal electrons at larger radii. The electron density profiles were inverted from interferometry measurements using 8 lines of sight.

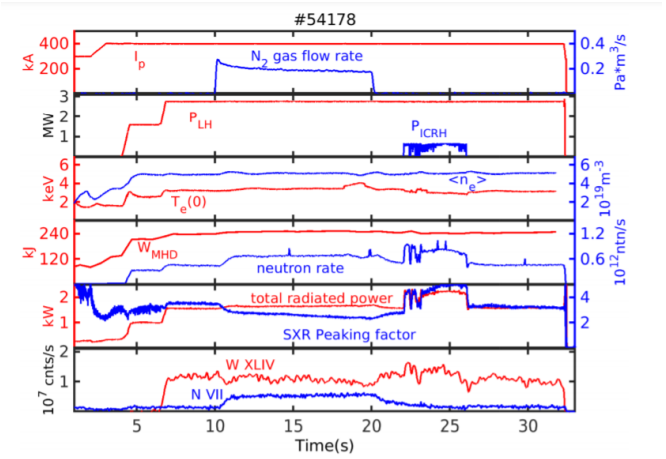

Figure 5: Time traces of several quantities for the WEST long pulse #54178.

Data consistency checks are performed with the METIS code [10] to compensate the lack of measurements such as the ion temperature profiles where the central Ti is made consistent with the measured DD neutron rate.

2.2. Predictive modelling of the electron temperature and density profiles

2.2.1. Flux driven modelling

Flux driven simulations are first considered using ASTRA with QuaLiKiz for the turbulent transport and NEO for the neoclassical transport. These simulations are carried out at 8 seconds during the Ip and LHCD plateaus, prior to the nitrogen injection phase. An off-axis LHCD power deposition has been assumed, at $\rho = 0.2$, with a Gaussian width of 0.3 and a current drive efficiency of 5×10^{18} A/W/m^2.

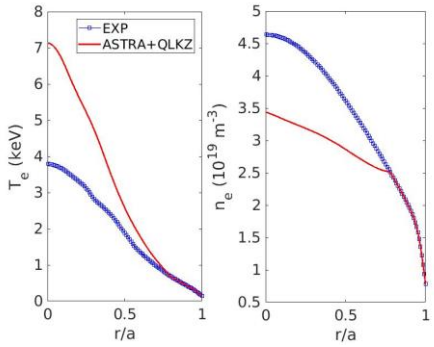

Figure 6: Predicted electron temperature and density profiles against experimental fitted profiles.

It is found (Fig. 6) that the electron temperature profile is overestimated while the density profile is underestimated. This results from low turbulent electron heat flux with respect to the electron temperature gradient due to stabilised Trapped Electron Modes.

2.2.2. Gradient driven modelling: collisional stabilisation of Trapped Electron Modes

To further investigate discrepancies observed in the flux driven simulations, gradient driven simulations are performed with the gyrokinetic codes QuaLiKiz and GKW [11]. Parameters for such simulations are gathered in Tab. 1. A quasilinear approach is adopted for the two code comparisons.

r/a	R/L_{T_e}	T_e/T_i	R/L_n	R/L_{T_i}	Z_{eff}	ν_*	$Q_e(\mathrm{kW/m^2})$	$Q_i(\mathrm{kW/m^2})$
0.5	15	1.8	**5.6**	**11.3**	2.8	0.5	46	15

Table 1: Parameters taken at 8 seconds and used for gradient driven simulations with QuaLiKiz and GKW.

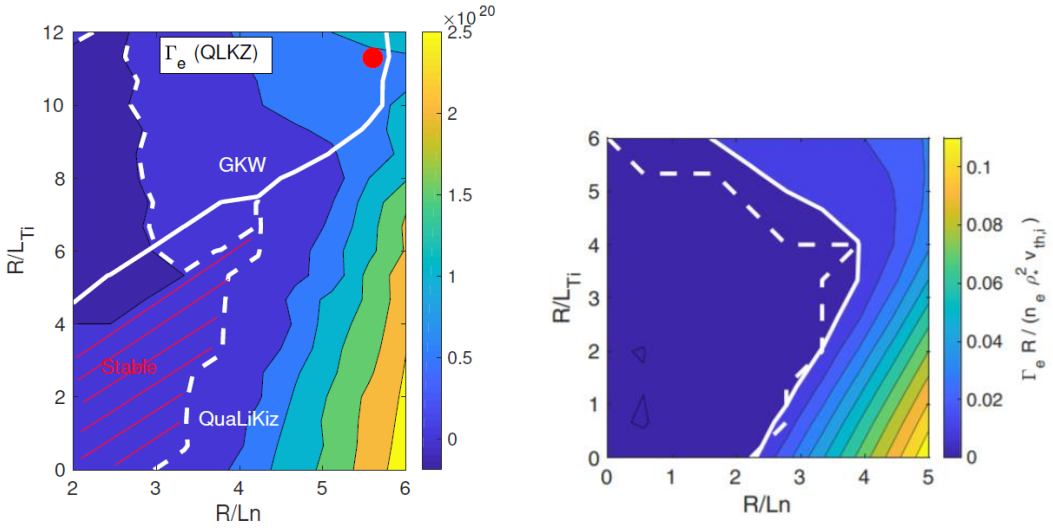

Figure 7: Comparison of the $\Gamma_e = 0$ condition between GKW (solid lines) and QuaLiKiz (dashed lines) for the nominal case (left) and a simpler case with $\frac{R}{LTe} = 0$ and the electron-ion collisionality $\nu = 0$ (right).

The particle flux is then computed and the condition $\Gamma_e = 0$ (no particle source and negligible Ware pinch) is found for the two codes and shown in the 2D space R/Ln and R/LTi in Fig. 7. While GKW recovers conditions close to the experimental R/Ln and R/LTi, QuaLiKiz finds much lower R/Ln fulfilling the condition $\Gamma_e = 0$. This is also consistent with the flux driven simulations where the modelled density peaking (with QuaLiKiz) was much lower than the experimental one. A collisionless case with reduced Trapped Electron Mode drive $\frac{R}{LTe} = 0$ is also investigated. In this case, a good agreement is found between GKW and QuaLiKiz for the condition $\Gamma_e = 0$. This underlines the role of the ∇Te TEM and collisions in the correct predictions of turbulent transport when dominant electron heating is used. Further development of the collision operator in QuaLiKiz have been performed [12] and preliminar results look promising in this strong TEM regime.

3. CONCLUSIONS

Reduced kinetic-theory-based models for transport modelling in view of plasma scenario optimisation and tungsten accumulation avoidance, are proven to be powerful and accurate tools. Applied to an ASDEX Upgrade discharge with NBI heating it was shown with ASTRA and QuaLiKiz that the competition between turbulent particle diffusion (enhanced with Te/Ti) and the central particle source from the neutral beams were the key ingredients for neoclassical tungsten accumulation modelling. The qualitative behaviour of the central density peaking with Te/Ti was also reproduced with faster transport models, i.e. QuaLiKiz 10DNN paving the way towards real-time tungsten transport predictions.

In specific regimes relevant for ITER operations, such as the ones encountered in the WEST tokamak, i.e. low toroidal rotation, dominant electron heating, additional development of reduced transport models are still required with constant validation against first principle modelling. Indeed, it was shown that in these regimes, a proper treatment of collisional stabilisation of Trapped Electron Modes are necessary

ACKNOWLEDGEMENTS

This work has been carried out within the framework of the EUROfusion Consortium and has received funding from the Euratom research and training programme 2014-2018 and 2019-2020 under grant agreement No 633053. The views and opinions expressed herein do not necessarily reflect those of the European Commission.

REFERENCES

[1] ANGIONI, C. et al, Nuclear Fusion **57** 056015 (2017)
[2] SERTOLI, M. et al, Physics of Plasmas **24** 112503 (2017)
[3] PEREVERZEV, G.V. et al, IPP-Report, IPP 5/98 (2002)
[4] BOURDELLE, C. et al, Plasma Physics and Controlled Fusion **58** 014036 (2016)
[5] BELLI, E. et al, Plasma Physics and Controlled Fusion **50** 095010 (2008)
[6] VAN DE PLASSCHE, K. et al, Physics of Plasmas **27** 022310 (2020)
[7] FELICI, F. et al, Nuclear Fusion **51** 083052 (2011)
[8] ANGIONI, C. et al, Physical Review Letters **90** 205003 (2003)
[9] YANG, X. et al, Nuclear Fusion **60** 086012 (2020)
[10] ARTAUD, J.F., Nuclear Fusion **58** 105001 (2018)
[11] PEETERS, A. et al, Computer Physics Communications **180** 2650 (2009)
[12] STEPHENS, C.D. et al, to be submitted